ISSN: 2993-5377

Research Article

Open Access Journal of Applied Science and Technology

Transcriptomic Insights into the Antitumor Mechanism of Bufalin in Hepatocellular Carcinoma Cell HepG2

Qinghang Song[2], Huhu Zhang[1], Ya Li[1] and Lina Yang[1*]

[1]*Department of Genetics and Cell Biology, Basic Medical College, Qingdao University, Qingdao 266071, China*

[2]*College of Medicine, Qingdao University, Qingdao 266071, China*

***Corresponding Author**
Lina Yang, Department of Genetics and Cell Biology, Basic Medical College, Qingdao University, Qingdao 266071, China.

Submitted: 2024, Feb 23; **Accepted:** 2024, Mar 29; **Published:** 2024, Apr 08

Citation: Song, Q., Zhang, H., Li, Y., Yang, L. (2024). Transcriptomic Insights into the Antitumor Mechanism of Bufalin in Hepatocellular Carcinoma Cell HepG2. *OA J Applied Sci Technol, 2*(2), 01-18.

Abstract

Aim: *Bufalin, a cardiotonic steroid derived from Chinese toad venom, exhibits anticancer effects against a variety of malignancies. However, its mechanism of action in human liver cancer remains elusive. This study aimed to elucidate the molecular underpinnings of bufalin's antitumor activity in HepG2 hepatocellular carcinoma (HCC) cells in vitro.*

Methods: *HepG2 cells were exposed to 40nM bufalin or 0nM bufalin as a control, and their transcriptomes were compared using RNA sequencing. Differentially expressed genes (DEGs) were identified and annotated, and enriched pathways were analyzed using Gene ontology, Kyoto Encyclopedia of Genes, Gene set enrichment analysis, and Genomes databases.*

Results: *RNA sequencing revealed 771 DEGs, comprising 362 upregulated and 409 downregulated genes. These DEGs were involved in 78 classical pathways, including 18 closely associated with cancer, such as central carbon metabolism in cancer, cell cycle, DNA replication, fatty acid metabolism, ferroptosis, and so forth. Eleven DEGs (Acyl-CoA oxidase 2 et al.) closely associated with HCC were validated by quantitative real-time reverse transcription-polymerase chain reaction, confirming their differential expressions in response to bufalin treatment.*

Conclusions: *This study demonstrated that bufalin modulates the expression of genes and pathways implicated in various aspects of HCC pathogenesis and progression, such as energy metabolism, cell proliferation, DNA replication, lipid oxidation, and cell death. These findings suggest that bufalin may exert its antitumor effect on HCC cells by targeting multiple molecular mechanisms, and provide potential targets for bufalin-based HCC therapy.*

Keywords: Bufalin, Hepatocellular Carcinoma, HepG2, Signaling Pathway, Transcriptome Analysis

1. Introduction

Liver cancer is a prevalent malignancy and ranks third among global cancer-related fatalities, following lung and colorectal cancers, with nearly 850,000 new patients diagnosed annually. It is also the third leading cause of cancer death, accounting for 8.2% of all cancer-related deaths [1, 2]. Liver cancer is typically associated with hepatocellular death and chronic liver injury caused by chronic alcohol abuse, viral hepatitis, chemical insults or drugs, aflatoxin-B1-contaminated food and obesity [3, 4]. Hepatocellular carcinoma (HCC) is the most usual type of liver cancer, representing more than 75% of all cases [5]. In spite of recent developments in treatment, Hepatocellular carcinoma (HCC) remains a challenging disease to manage, especially in its advanced stages. Current treatment options include liver transplantation, chemotherapy, surgical resection and local ablation, but these approaches are often limited by their efficacy and side effects. Sorafenib, a multikinase inhibitor, is the first-line systemic therapy approved by the FDA for advanced HCC, but its response rate is modest and its benefits are often short-lived [6]. Other molecularly targeted therapies, such as cabozantinib, lenvatinib, and regorafenib, have been approved for later treatment or second-line of HCC, but they offer only modest survival benefits [7-9]. Consequently, it's crucial to develop innovative and effective drug to target HCC cells.

Bufalin, a potent anticancer agent derived from Chinese toad venom (Chansu), has been applied for various purposes in traditional Chinese medicine, such as pain management, anti-inflammation, and antineoplasia [10]. Bufalin and its derivatives belong to the class of cardiotonic steroids, which can target multiple molecular pathways in cancer cells, including Na+/K+-ATPase, NF-κB, Wnt/β-catenin, PI3K/Akt, MAPK, STAT3, p53, and others [11]. Previous studies have shown that bufalin prevents cancer proliferation, invasion and migration via inducing different cell death mechanisms such as apoptosis, necrosis, and autophagy [12-14]. Bufalin regulates metastasis

formation by blocking angiogenesis and reducing cancer cell stemness [15]. Bufalin also affects the immune microenvironment by reversing various drug resistance mechanisms [16]. Bufalin and its derivatives have shown anticancer activity against various types of human cancers, such as colorectal cancer, hepatocellular carcinoma, lung cancer, pancreatic cancer, breast cancer, ovarian cancer, prostate cancer and leukemia [17-26]. Bufalin and its derivatives have been experienced in animal models and clinical trials, showing promising results in terms of safety and efficacy. These studies approve bufalin becoming a very auspicious novel anti-cancer drug candidate. However, the transcriptome alterations induced by bufalin in HCC cells have not been well explored. To fill this knowledge gap, our study used RNA sequencing to investigate the effect of bufalin on the gene expression profile of HepG2 cells, a human liver cancer cell line. Our analysis revealed differentially expressed genes and pathways that could explain anti-cancer mechanisms of bufalin and provide potential targets for liver cancer therapy.

2. Materials and Methods

2.1 Cell Lines and Cell Culture

HepG2 cells were obtained from the Type Culture Collection of the Yubo Biology (Shanghai, China). Cells were cultured in DMEM medium supplemented with 10% fetal bovine serum (FBS) at 37°C in a humidified incubator with 5% CO2. The culture medium was refreshed every 2 days. All cell culture experiments were performed within 10 passages after thawing.

2.2 Chemicals and Reagents

We obtained Dulbecco's modified Eagle's medium (DMEM), fetal bovine serum (FBS), and trypsin-ethylenediaminetetraacetic acid (EDTA) from Gibco. TRIzol reagent, protease inhibitors, and Cell Counting Kit-8 (CCK-8) assay were purchased from Thermo Fisher Scientific. Bufalin was obtained from Selleck. SYBR Green polymerase chain reaction (PCR) Master Mix was purchased from Vazyme. TransScript All-in-One First-Strand cDNA Synthesis SuperMix was obtained from TRANSGEN BIOTECH.

2.3 Total RNA Extraction

We seeded 1.5 × 105 HepG2 cells per well in six-well plates and starved them for 24 hours before treating them with 0 or 40 nM bufalin for 48 hours. Next, we extracted total RNA using TRIzol reagent according to the manufacturer's instructions. We then assessed RNA purity and concentration using a NanoPhotometer spectrophotometer (IMPLEN, CA, USA) and a Qubit 3.0 Fluorometer (Life Technologies, USA), respectively. Finally, we confirmed RNA integrity using an Agilent 2100 RNA Nano 6000 Assay Kit. All samples passed quality control with an RNA integrity number (RIN) of at least 8.0.

2.4 RNA Sequencing and Library Construction

ANOROAD (Beijing, China) performed RNA sequencing on six cDNA libraries, three from the 40 nM bufalin group and three from the control group. The cDNA libraries were constructed after quality control, and the qualified libraries were sequenced on an Illumina Hiseq platform.

2.5 Data Analysis

Raw reads were preprocessed by filtering out low-quality reads, trimming adapter sequences, and removing reads rich in poly-N nucleotides. Cufflinks v2.1.1 was then used to identify differentially expressed genes (DEGs) between the bufalin and control groups. Transcript abundance, a proxy for gene expression levels, was quantified using fragments per kilobase of exon model per million mapped fragments (FPKM). DEGs were identified using Cuffdiff software based on the following three criteri) log2 fold change (FC) > 1 or < −1) q-value false discovery rate (FDR) < 0.0) FPKM value > 1.

2.6 Functional Enrichment Analysis

To identify significantly enriched biological processes, gene ontology (GO) functional enrichment analysis was performed using the GOseq R package. DEGs were compared to the genomic background, and GO terms with a corrected p-value of less than 0.05 were considered to be significantly enriched. Kyoto Encyclopedia of Genes and Genomes (KEGG) pathway enrichment analysis was also performed using KOBAS software to identify significantly enriched KEGG pathways compared to the transcriptome background through a hypergeometric test (hypergeometric $p < 0.05$).

2.7 Gene Set Enrichment Analysis

Differential expression analysis was performed using DESeq2 v1.28.1 to identify genes that were differentially expressed between the bufalin and control groups. Gene expression levels were normalized using regularized-logarithm transformation, and heat maps were generated to visualize the expression patterns of differentially expressed genes (FDR p-values < 0.05).

Gene set enrichment analysis (GSEA) was performed using the clusterProfiler package to identify groups of genes that were coordinately upregulated or downregulated in response to bufalin treatment. GSEA was conducted using 10,00 permutations, and gene sets ranging from 10 to 1,000 genes were considered. Gene sets with an adjusted p-value (p.adj) of less than 0.05, a false discovery rate (FDR) of less than 0.25, a normalized enrichment score (NES) greater than 1.5, and the species Homo sapiens were considered to be significantly enriched. The following gene sets were included in the analysis: Canonical pathways gene sets (including gene sets from the KEGG (Kanehisa, 2000) and WikiPathways (Martens et al., 2021) pathway databases), Hallmark gene sets (Liberzon et al., 2015) and Oncogenic signature gene sets (Liberzon et al., 2011) [27].

2.8 Quantitative Real-Time Polymerase Chain Reaction Analysis of Gene Expression

To validate the RNA sequencing results and further investigate the expression of specific genes, qRT-PCR was performed to quantify the mRNA levels of selected genes in HepG2 cells treated with bufalin for 48 hours. Glyceraldehyde-3-phosphate dehydrogenase (GAPDH) was used as a reference gene for normalization. The primer sequences for the target and reference genes are listed in Table 1. Total RNA (1 μg) was extracted from bufalin-treated HepG2 cells using Trizol reagent and reverse transcribed into cDNA using an RT reagent kit. qRT-PCR was

performed in a 10 µl reaction mixture containing 5 µl AceQ qPCR SYBR Green Master Mix, 0.2 µM of each primer, 0.31 µl cDNA template, and 4.29 µl nuclease-free water. The following thermal cycling conditions were used: 95°C for 5 minutes, followed by 40 cycles of 95°C for 10 seconds and 60°C for 30 seconds. The fold change of target gene expression was calculated using the comparative threshold cycle (Ct) method, with GAPDH as the reference gene. The formula is as follows:

Fold change = $2^{-\Delta\Delta Ct}$.

Gene	Forward primer	Reverse primer
PFKFB4	5′- TTGGAGAACAGAATGGCTACAA-3′	5′- CGTAGGAGTTCTCATAGCACTC-3′
MCM6	5′-TCGGGCCTTGAAAACATTCGT-3′	5′-TGTGTCTGGTAGGCAGGTCTT-3′
HK2	5′- CGACAGCATCATTGTTAAGGAG-3′	5′- GCAGGAAAGACACATCACATTT-3′
ACOX2	5′- CCCAGTGACCCAGAGGCAAAG-3′	5′-CTTGGTTCAGAATGGCAGTGTAGG-3′
FZD4	5′- GGTGTTCTCAGTACTGTACACA-3′	5′- GCCCACCAACAAAGACATAAAA-3′
AKR1B1	5′- ACGCATTGCTGAGAACTTTAAG-3′	5′- TTCCTGTTGTAGCTGAGTAAGG-3′
SERPINE2	5′- GTGATGAGATACGGCGTAAATG-3′	5′- TTCTTAACAAACACGGCGTTAG-3′
ACSL4	5′- ACCAGGGAAATCCTAAGTGAAG-3′	5′- GGTGTTCTTTGGTTTTAGTCCC-3′
ADH4	5′- GAACATTCTTTGGTGGTTGGAA-3′	5′- TTTTGTCAAAAGGCAGGGTATG-3′
IDH1	5′- CACCAACGACCAAGTCACCAAG-3′	5′- ACTCCTCAACCCTCTTCTCATCAG-3′
CPT2	5′- GCCTAGATGACTTCCCCATTAA-3′	5′- AAAGGATTTATCAAACCAGCGG-3′

TABLE 1: List of Gene Primers.

2.9 Statistical Analysis

Data were expressed as mean ±SD of independent experiments repeated three times under the same conditions. Statistical analyses were performed with GraphPad Prism 9.0 software or Excel (Microsoft) using a two-tailed Student's t test. Except for box plots, all other statistic data show mean ± SEM of at least three biologically independent experiments or samples. Multiple group comparisons were performed using one-way analysis of variance (ANOVA). P value less than 0.05 was considered significant.

3. Results

3.1 Bufalin Inhibits the Proliferation of HepG2 Cells

Aforementioned studies have revealed that bufalin has an inhibiting effect in various cancer cells [10, 11, and 28]. To assess the impact of bufalin on HCC cell proliferation, we performed a CCK-8 assay on HepG2 cells treated with different concentrations of bufalin (0, 25, 50, 100, 200, 400, and 800 nM). We found that bufalin significantly inhibited HepG2 cell proliferation in a dose- and time-dependent manner (Figure 1A). Based on the results, we determined the subsequent optimal treatment concentration to be 40 nM

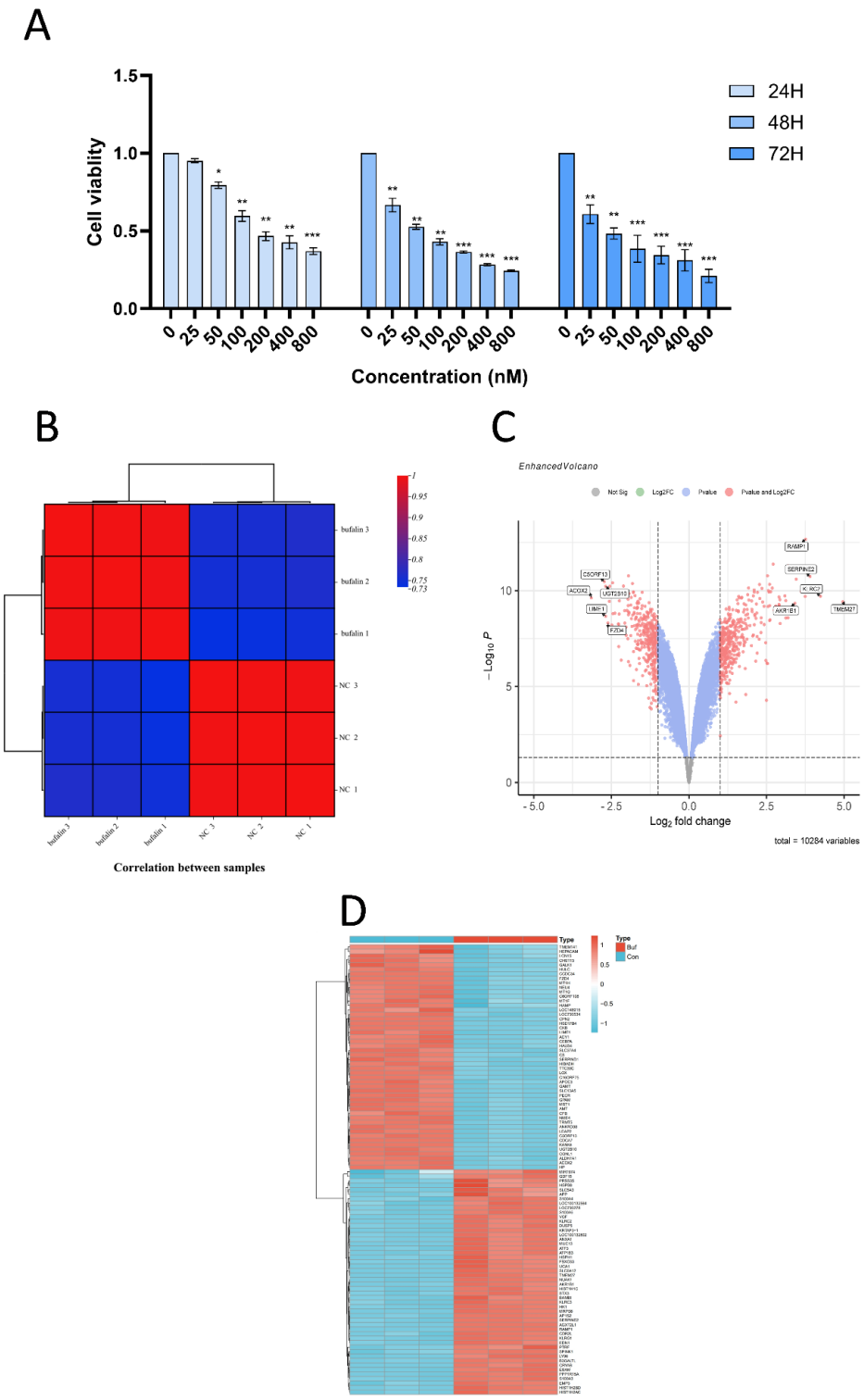

Figure 1: Effects of bufalin on HepG2 cell growth. (A) Bufalin inhibited HepG2 cell proliferation in a dose- and time-dependent manner, as measured by the Cell Counting Kit-8 (CCK-8) assay. Data are presented as the mean ± standard deviation of five independent experiments performed in triplicates. *p < 0.05, **p < 0.01, ***p < 0.001 versus control without bufalin. (B) Correlation coefficient plot. A higher correlation coefficient indicates a higher correlation between two samples. (C) Volcano map of differentially expressed genes. The plot depicts the log2 fold change of differentially expressed genes between the treatment and control groups on the x-axis and the negative log10 of the adjusted p-value on the y-axis. Each point represents a gene, with red points indicating significantly up- and downregulated genes and gray dots indicating genes with no significant difference in expression (FC > 1 and adjusted p-value < 0.05). (D) Hierarchical clustering heat map of differentially expressed genes in bufalin-treated and control HepG2 cells. This heat map depicts the results of a hierarchical clustering analysis of differentially expressed genes, with red and blue indicating up- and downregulated genes, respectively.

3.2 RNA Sequencing Reveals the Transcriptomic Landscape of Bufalin-Treated HepG2 Cells

To further elucidate the molecular basis of bufalin's antitumor activity in HepG2 cells, we performed RNA sequencing to compare the transcriptomes of bufalin-treated and untreated cells. We obtained a total of 36.85 Gb of high-quality reads, with a mapping rate of 98.15-98.56%. We identified 771 DEGs between the two groups, with 362 upregulated and 409 downregulated (Figures 1B-D). The DEGs were involved in a variety of signaling pathways related to cell communication, cell adhesion, cell cycle, DNA replication, blood vessel morphogenesis, positive regulation of phosphorylation and extracellular matrix organization (Tables 2, 3).

Gene name	Gene description	log2FoldChange	Adjusted P-value
ACOX2	Acyl-CoA oxidase 2, branched chain	-3.148114	5.45E-08
C5ORF13	Chromosome 5 open reading frame 13	-2.729210898	3.50E-08
UGT2B10	UDP glucuronosyltransferase family 2 member B10	-2.686869125	3.61E-08
LIME1	Lck interacting transmembrane adaptor 1	-2.68545044	1.72E-07
FZD4	Frizzled class receptor 4	-2.610266111	2.68E-07
KANK4	KN motif and ankyrin repeat domains 4	-2.595782991	2.15E-08
CDCA7	Cell division cycle associated 7	-2.56742891	4.62E-08
SLC13A5	Solute carrier family 13 member 5	-2.565367222	6.58E-08
LOX	Lysyl oxidase	-2.551645088	3.61E-08
HP	Haptoglobin	-2.528846852	5.06E-08
CHST13	Carbohydrate sulfotransferase 13	-2.486206861	2.99E-07
ANKRD38	Ankyrin repeat domain 38	-2.462417884	3.55E-08
MST1	Macrophage stimulating 1	-2.452352866	1.44E-07
SLC37A4	Solute carrier family 37 member 4	-2.384998056	1.42E-07
NEU4	Neuraminidase 4	-2.279091181	2.82E-07
HULC	Highly upregulated in liver cancer	-2.264888491	2.88E-07
MT1G	Metallothionein 1G	-2.262334625	1.41E-06
CEBPA	CCAAT/enhancer binding protein alpha	-2.253367894	1.45E-07
LEAP2	Liver expressed antimicrobial peptide 2	-2.243523384	6.48E-08
TMEM141	Transmembrane protein 141	-2.185113011	4.04E-06

TABLE 2: Twenty Significantly Upregulated genes linked to Cancer in Huh-7 cells Treated with Metformin.

Gene name	Gene description	log2FoldChange	Adjusted P-value
TMEM27	Transmembrane protein 27	4.960380278	6.81E-08
KLRC2	Killer cell lectin-like receptor C2	4.238154028	5.21E-08
SERPINE2	Serpin family E member 2	3.903513389	2.39E-08
RAMP1	Receptor activity modifying protein 1	3.759223139	2.18E-09
LOC100132802	Uncharacterized LOC100132802	3.745003806	5.21E-08
KRTAP3-1	Keratin-associated protein 3-1	3.620452215	4.28E-08
ESAM	Endothelial cell-selective adhesion molecule	3.563188398	1.83E-08
S100A3	S100 calcium-binding protein A3	3.455497343	2.93E-08
AKR1B1	Aldo-keto reductase family 1 member B1	3.416861444	7.54E-08
UCA1	Urothelial cancer-associated 1	3.192879898	1.89E-07
MRPS6	Mitochondrial ribosomal protein S6	3.192419806	1.82E-08
ATF3	Activating transcription factor 3	3.123393407	1.90E-07
HIST1H2AC	Histone cluster 1 H2A family member c	3.122156806	6.42E-08
SLC6A12	Solute carrier family 6 member 12	3.092487	5.21E-08
KLRC3	Killer cell lectin-like receptor C3	2.938106528	2.74E-07
LY96	Lymphocyte antigen 96	2.932915407	6.13E-08

CDR2L	Cerebellar degeneration-related protein 2-like	2.903871796	8.19E-08
EDN1	Endothelin-1	2.901588317	8.10E-08
KLRG1	Killer cell lectin-like receptor G1	2.901014963	5.40E-08
EMP3	Epithelial membrane protein 3	2.799581278	8.79E-08

TABLE 3: Twenty significantly downregulated genes linked to cancer in Huh-7 cells treated with metformin.

4. Function Enrichment Analysis: Unveiling Key Genes Functions

To explore functional changes of gene expression related with bufalin-treated in HepG2 cell, we performed GO enrichment analysis of the 771 DEGs from the library. We identified 1341 enriched GO terms ($q < 0.05$), including 110 in cellular components ,152 in molecular functions and 1079 in biological processes. Notably, the significantly enriched biological processes included small molecule catabolic process, carboxylic acid biosynthetic process, organic acid cataboli, carboxylic acid cataboli, cellular lipid catabolic, steroid metabolic process, response to metal ion, alpha-amino acid metabolic and organic acid biosynthetic process (Figure 2, Table 4).

To further explore the functional consequences of bufalin treatment, we performed GO enrichment analysis of the upregulated and downregulated DEGs separately. Downregulated genes were significantly enriched in 992 GO terms ($q < 0.05$), including 781 in biological processes, 103 in cellular components, and 108 in molecular functions. The top ranking categories in the biological process included transferrin transport, cellular monovalent inorganic cation homeostasis, monovalent inorganic cation homeostasis, pH reduction, iron ion transport, and regulation of pH (Figure 3 and Table 5). These findings suggest that bufalin treatment disrupts a variety of essential cellular processes, such as metal ion transport, pH regulation, and iron metabolism. Upregulated genes were significantly enriched in 742 GO terms ($q < 0.05$), including 599 in biological processes, 46 in cellular components, and 97 in molecular functions. The top ranking categories in the biological process with upregulated genes included NAD binding, NAD or NADP as acceptor, acting on CH-OH group of donors, organic acid binding, oxidoreductase activity, carboxylic acid binding, and carbohydrate kinase activity (Figure 4 and Table 6). These findings suggest that bufalin treatment induces metabolic changes, such as increased oxidation and carbohydrate metabolism, which may also contribute to its antitumor activity. Of note, the enrichment degree of small molecule catabolic process was the highest among all the GO terms, suggesting that bufalin treatment promotes the breakdown of small molecules, which may be a key mechanism of its antitumor activity.

ID	Description	GeneRatio	p.adjust
GO:0044282	small molecule catabolic process	62/703	2.21837E-15
GO:0016054	organic acid catabolic process	40/703	5.63269E-10
GO:0046395	carboxylic acid catabolic process	40/703	5.63269E-10
GO:0044242	cellular lipid catabolic process	33/703	6.28674E-08
GO:0008202	steroid metabolic process	40/703	6.28674E-08
GO:0010038	response to metal ion	42/703	6.50807E-08
GO:1901605	alpha-amino acid metabolic process	30/703	6.50807E-08
GO:0046394	carboxylic acid biosynthetic process	42/703	6.50807E-08
GO:0016053	organic acid biosynthetic process	42/703	6.50807E-08
GO:0016042	lipid catabolic process	39/703	3.0523E-07

TABLE 4: List of 10 biological process entries for all differentially expressed genes.

ID	Description	GeneRatio	p.adjust
GO:0033572	transferrin transport	9/305	8.88825E-06
GO:0030004	cellular monovalent inorganic cation homeostasis	14/305	8.88825E-06
GO:0055067	monovalent inorganic cation homeostasis	16/305	8.88825E-06
GO:0045851	pH reduction	10/305	2.7449E-05
GO:0006826	iron ion transport	11/305	4.44897E-05
GO:0006885	regulation of pH	12/305	6.08678E-05
GO:0043312	neutrophil degranulation	26/305	6.08678E-05
GO:0002283	neutrophil activation involved in immune response	26/305	6.08678E-05
GO:0016236	macroautophagy	20/305	7.30202E-05

GO:0016241	regulation of macroautophagy	15/305	7.30202E-05

TABLE 5: List of 10 biological process entries for upregulating differentially expressed genes.

ID	Description	GeneRatio	p.adjust
GO:0044282	small molecule catabolic process	47/293	6.886E-22
GO:0016054	organic acid catabolic process	32/293	1.29861E-15
GO:0046395	carboxylic acid catabolic process	32/293	1.29861E-15
GO:1901605	alpha-amino acid metabolic process	23/293	7.7697E-11
GO:0044242	cellular lipid catabolic process	24/293	2.12882E-10
GO:0006066	alcohol metabolic process	30/293	2.12882E-10
GO:0072329	monocarboxylic acid catabolic process	19/293	2.12882E-10
GO:0016042	lipid catabolic process	28/293	3.29657E-10
GO:1901606	alpha-amino acid catabolic process	16/293	2.11074E-09
GO:0006520	cellular amino acid metabolic process	26/293	7.80913E-09

TABLE 6: List of 10 biological process entries for downregulating differentially expressed genes.

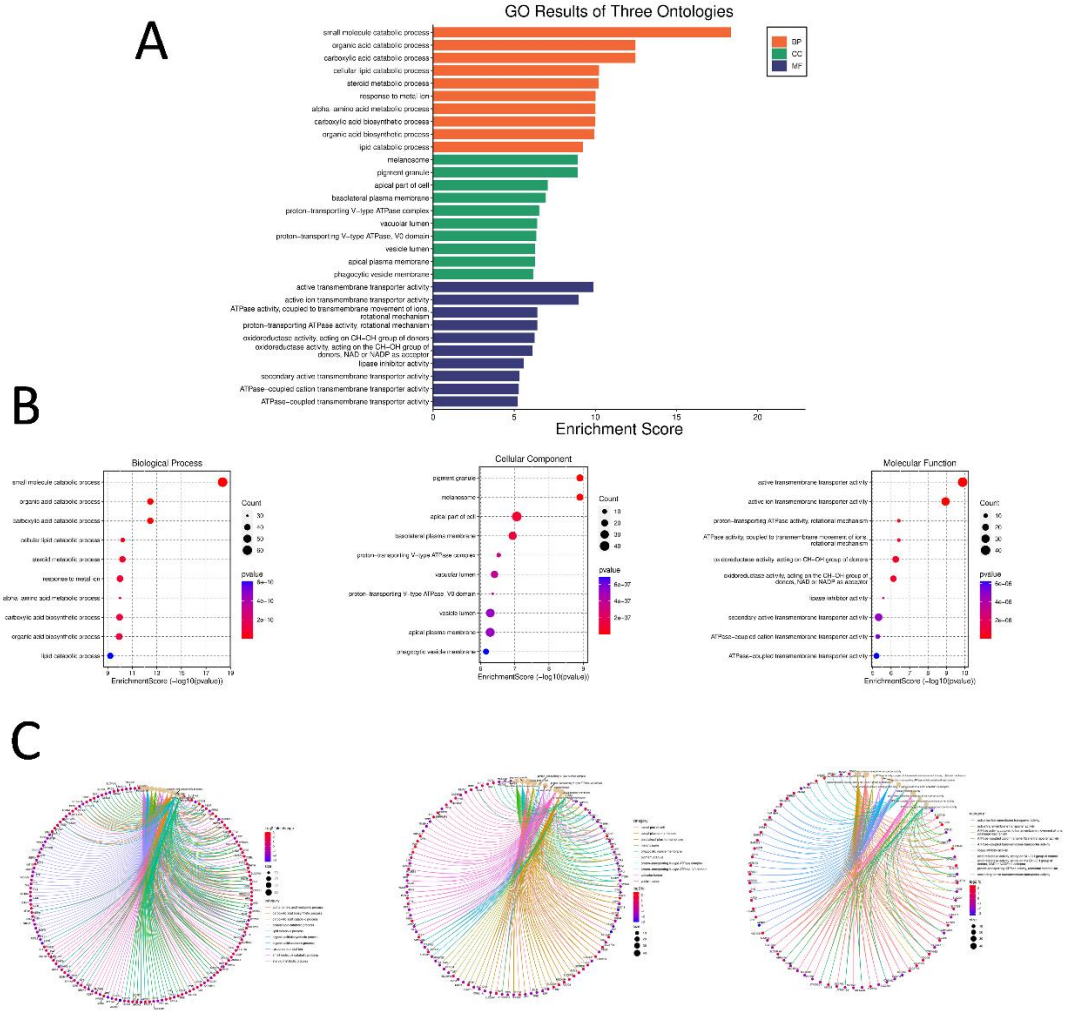

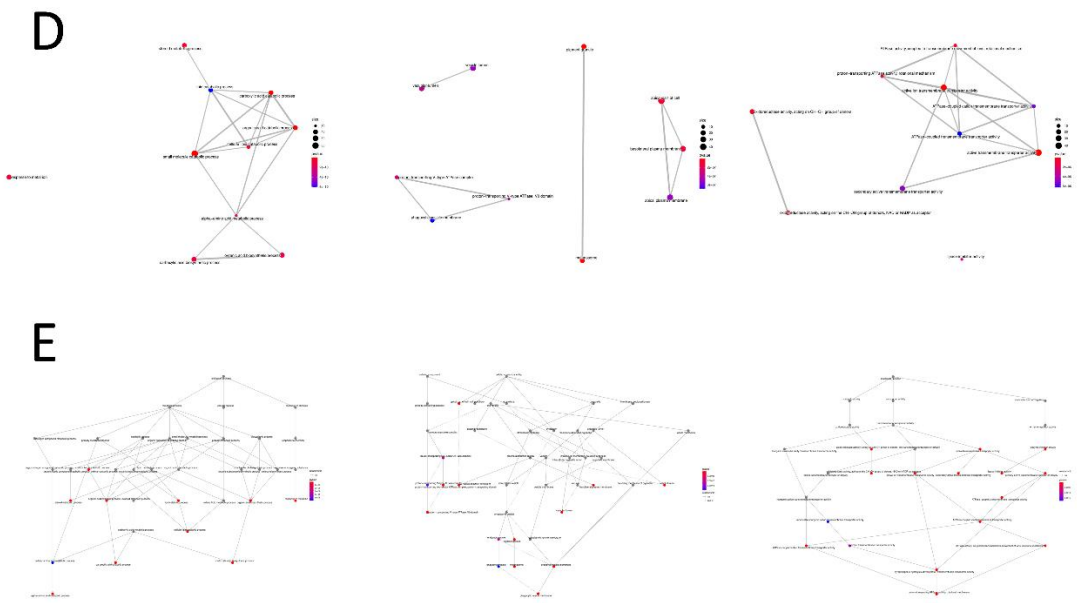

Figure 2: GO enrichment analysis of differentially expressed genes in treating with bufalin HepG2. (A) GO function analysis histogram of all DEGs between the bufalin treatment and control groups. BP is marked by sienna; CC is marked by dark cyan and MF is marked by steel blue. (B) All DEG GO analysis's bubble chart. Bubble charts visualize the GO terms enriched in the DEGs, with the x-axis representing the enrichment factor and the y-axis representing the GO terms. The enrichment factor is a measure of the degree to which a GO term is overrepresented in the DEGs compared to the background genome. A higher enrichment factor indicates a greater overrepresentation of the GO term in the DEGs. The size of each bubble represents the number of genes in the GO term, and the color of the bubble corresponds to the p-value of the enrichment. A lower p-value indicates a more statistically significant enrichment. (C) Gene-Concept Network of all DEGs. (D) Enrichment Map on all DEGs (E) Directed acyclic graph on all DEGs. The DAG is a visualization of the GO enrichment results, with each node representing a GO term and the edges representing relationships between GO terms. The direction of each edge indicates the hierarchical relationship between the corresponding GO terms.

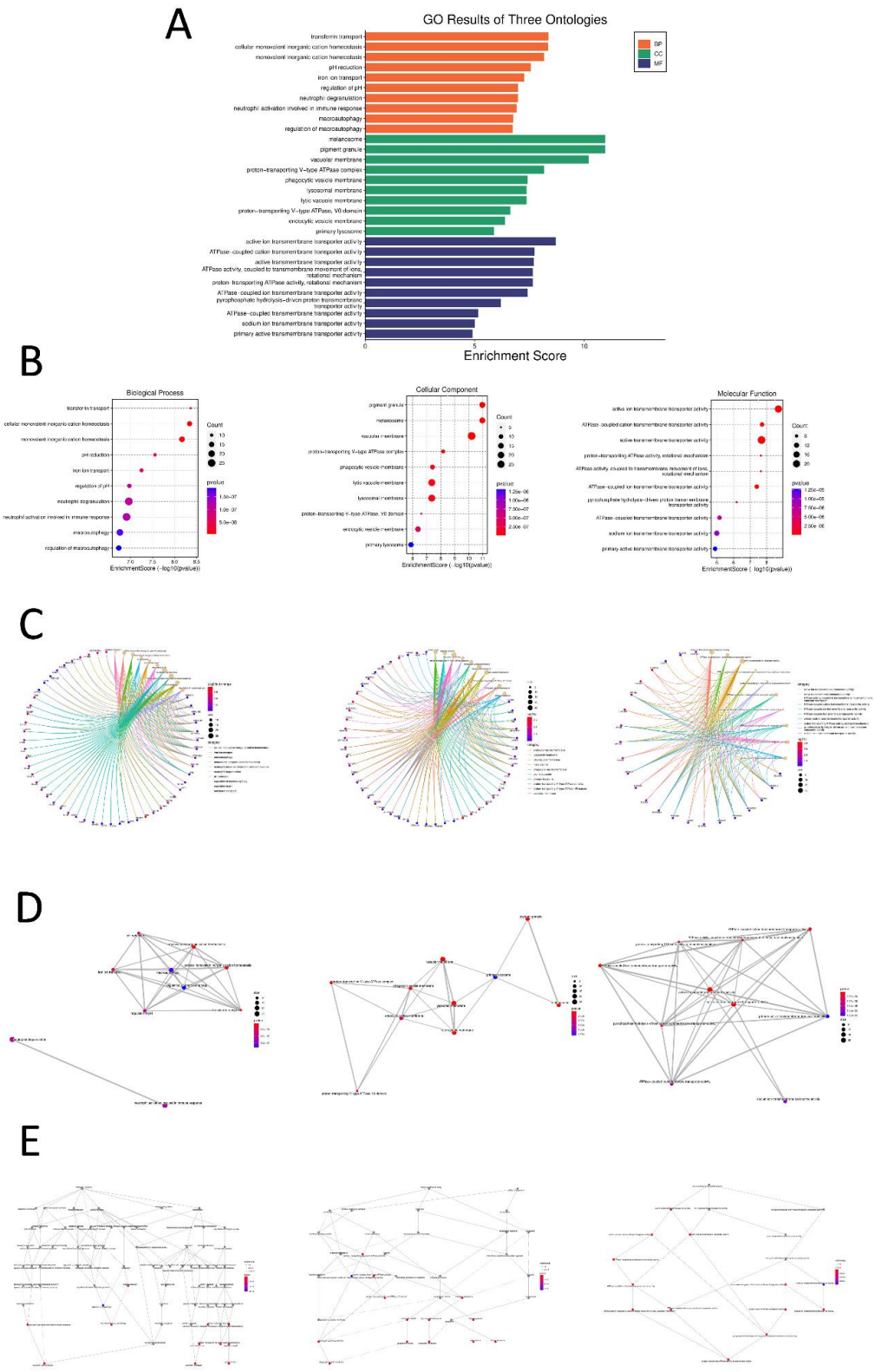

Figure 3: (A) GO function analysis histogram of upregulated DEGs. BP is marked by sienna; CC is marked by dark cyan and MF is marked by steel blue. (B) Upregulated DEG GO analysis's bubble chart. (C) Gene-Concept Network of upregulated DEGs. (D) Enrichment Map on upregulated DEGs. (E) Directed acyclic graph of upregulated DEGs.

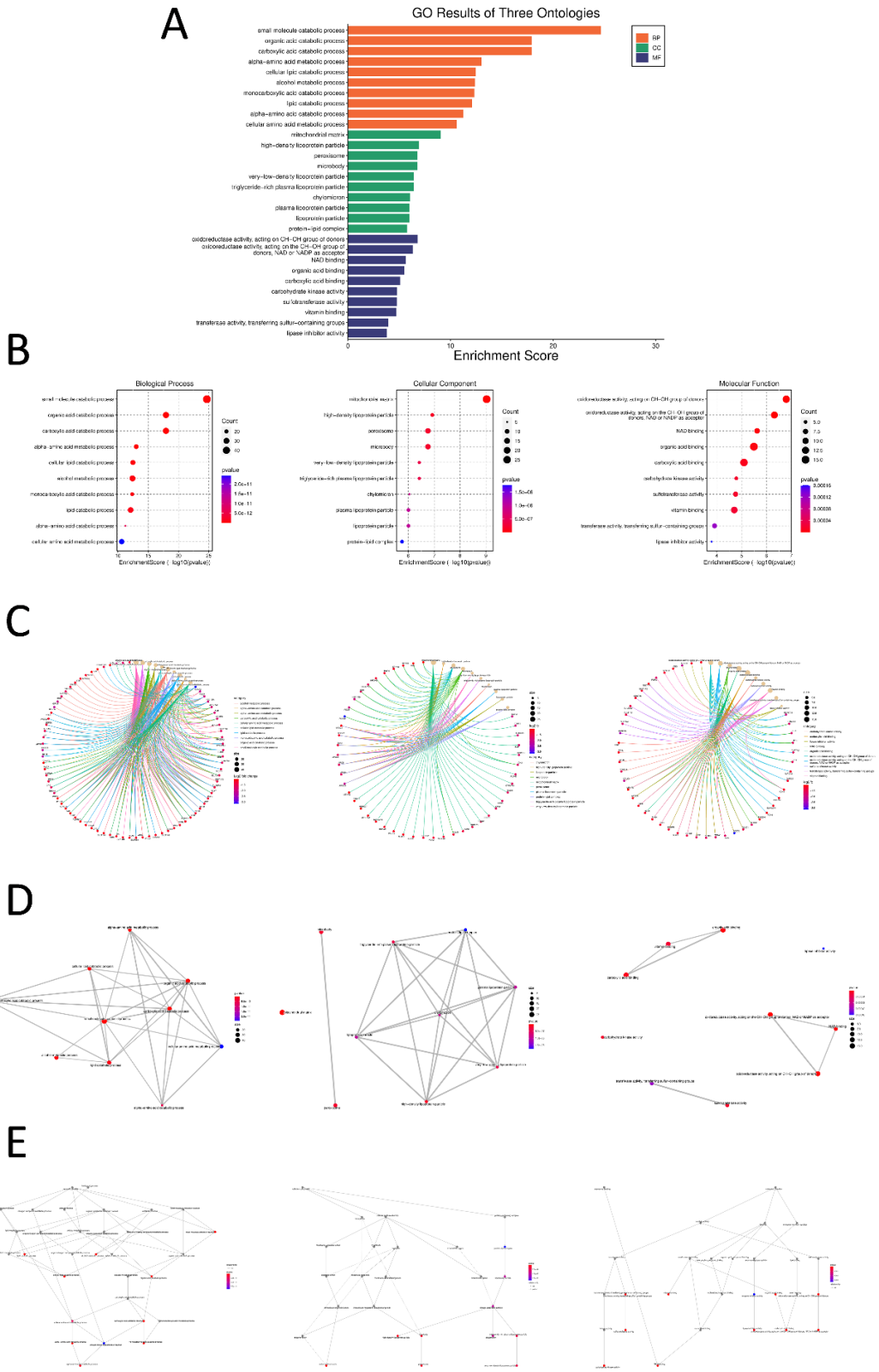

Figure 4: (A) GO function analysis histogram on downregulated DEGs. BP is marked by sienna; CC is marked by dark cyan and MF is marked by steel blue. (B) Bubble chart of downregulated DEG GO analyses. (C) Gene-Concept Network on downregulated DEGs. (D) Enrichment Map on downregulated DEGs. (E) Directed acyclic graph on upregulated DEGs.

Coordinating gene activity is essential for biological function in organisms, and pathway analysis can help us to elucidate these complex interactions. To identify the molecular mechanisms underlying bufalin's effects on HepG2 cells, we performed KEGG enrichment analysis on the 771 DEGs. This analysis revealed significant enrichment ($p < 0.05$) for 78 KEGG pathways, including Lysosome, Phagosome, Chemical carcinogenesis - receptor activation, Carbon metabolism, Peroxisome, FoxO signaling pathway, AMPK signaling pathway, Complement and coagulation cascades, Cell cycle, Fatty acid metabolism, PPAR signaling pathway, and Glycolysis/Gluconeogenesis (Figures 5A and B, Table 7). The 362 upregulated genes were significantly enriched in 51 KEGG pathways ($p < 0.05$) (Figures 5C, D, and Table 8), including Lysosome, Mitophagy - animal, Autophagy - animal, and Galactose metabolism, Ferroptosis, Fructose and mannose mTOR signaling pathway, metabolism and so on. The 409 downregulated genes were significantly enriched in 56 KEGG pathways ($p < 0.05$) (Figures 5E, F and Table 9), which included Carbon metabolism, Peroxisome, Glycine, serine and threonine metabolism, Glyoxylate and dicarboxylate metabolism, Complement and coagulation cascades, Fatty acid degradation, Metabolism of xenobiotics by cytochrome P450, Glycolysis / Gluconeogenesis, Tyrosine metabolism, PPAR signaling pathway, DNA replication and so on. In these pathways, we paid most attention to these pathways, such as Fatty acid metabolism, Glycolysis / Gluconeogenesis, Cell cycle, and Ferroptosis.

ID	Description	GeneRatio	p.adjust	Count
hsa04146	Peroxisome	17/425	0.000220509	17
hsa05204	Chemical carcinogenesis - DNA adducts	15/425	0.000265236	15
hsa04142	Lysosome	21/425	0.000367249	21
hsa04964	Proximal tubule bicarbonate reclamation	8/425	0.000920101	8
hsa00052	Galactose metabolism	9/425	0.001082358	9
hsa01200	Carbon metabolism	18/425	0.001082358	18
hsa01230	Biosynthesis of amino acids	14/425	0.001082358	14
hsa00051	Fructose and mannose metabolism	9/425	0.001201708	9
hsa00980	Metabolism of xenobiotics by cytochrome P450	14/425	0.001333396	14
hsa04966	Collecting duct acid secretion	8/425	0.001387673	8

TABLE 7: List of 10 KEGG analyses of all differentially expressed genes.

ID	Description	GeneRatio	p.adjust	Count
hsa04142	Lysosome	19/169	4.62592E-09	19
hsa05323	Rheumatoid arthritis	12/169	4.93289E-05	12
hsa05120	Epithelial cell signaling in Helicobacter pylori infection	10/169	0.000122748	10
hsa04145	Phagosome	14/169	0.000169417	14
hsa04721	Synaptic vesicle cycle	10/169	0.00020277	10
hsa05110	Vibrio cholerae infection	8/169	0.000301929	8
hsa04966	Collecting duct acid secretion	6/169	0.000531885	6
hsa04137	Mitophagy - animal	8/169	0.00343887	8
hsa04140	Autophagy - animal	11/169	0.004228353	11
hsa00052	Galactose metabolism	5/169	0.009938568	5

TABLE 8: List of 20 KEGG analyses of upregulated differentially expressed genes.

ID	Description	GeneRatio	p.adjust	Count
hsa01200	Carbon metabolism	15/192	1.53921E-05	15
hsa04146	Peroxisome	11/192	0.000192185	11
hsa00260	Glycine, serine and threonine metabolism	8/192	0.000192185	8
hsa05204	Chemical carcinogenesis - DNA adducts	10/192	0.000192185	10
hsa00630	Glyoxylate and dicarboxylate metabolism	7/192	0.000192185	7
hsa04610	Complement and coagulation cascades	11/192	0.000192185	11
hsa01230	Biosynthesis of amino acids	10/192	0.000310303	10
hsa00980	Metabolism of xenobiotics by cytochrome P450	10/192	0.000387875	10

hsa00071	Fatty acid degradation	7/192	0.001530944	7
hsa00330	Arginine and proline metabolism	7/192	0.003252439	7

TABLE 9: List of 10 KEGG analyses of downregulated differentially expressed genes.

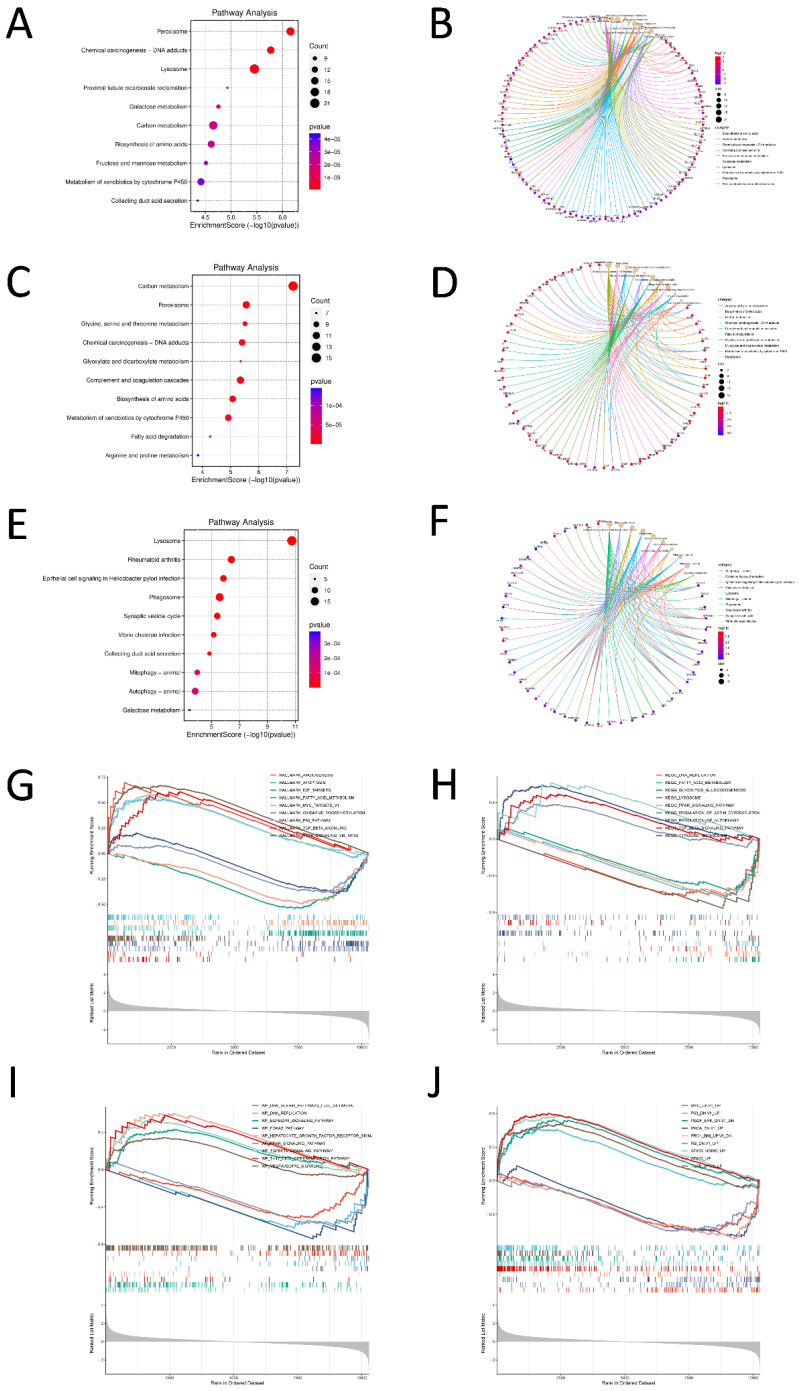

Figure 5: DEGs' GSEA and KEGG enrichment analysis. (A) All DEGs' bubble chart about KEGG. The y-axis represents the KEGG pathways and the x-axis represents the enrichment factor, which is a measure of the degree to which a KEGG pathway is overrepresented in the DEGs compared to the background genome. A higher enrichment factor indicates a greater overrepresentation of the KEGG pathway in the DEGs. The dot size represents the number of genes in the KEGG pathway, and the dot color corresponds to the p-value of the enrichment. A lower p-value indicates a more statistically significant enrichment. (B) Gene-Concept Network on all DEGs. (C) Upregulated DEGs' bubble chart of about KEGG enrichment analysis. (D) Gene-Concept Network on upregulated DEGs. (E) Downregulated DEGs' bubble chart about KEGG. (F) Gene-Concept Network on downregulated DEGs. (G-K)GSEA enrichment plots of the top 9 Hallmark Gene Sets Related with Cancer (G), top 9 KEGG gene sets Related with Cancer (H), top 9 Wiki Pathways gene sets Related with Cancer (I), and top 9 Oncogenic gene sets Related with Cancer (K).

5. Pathway Insights through GSEA

GSEA (gene set enrichment analysis) is a powerful tool for identifying signaling pathways that are differentially regulated in different biological conditions. We executed GSEA to analyze the DEGs between HepG2 cells treated with 40nM bufalin and those treated with 0nM bufalin. We used four gene set collections from MSigDB: The Hallmark, KEGG, WikiPathways, and Oncogenic signature gene sets. Our primary focus was on identifying gene sets with notable Normalized Enrichment Scores (NES) that were associated with cancer-related processes. From each of these four analyses, we systematically selected the top 10 gene sets based on their high NES values and their relevance to cancer biology. This rigorous approach allowed us to pinpoint gene sets that exhibited robust enrichment patterns in our differential gene dataset, shedding light on potential molecular pathways and mechanisms underlying cancer pathogenesis. The results are summarized in Table 10, 11, 12, 13.

ID	setSize	enrichmentScore	NES	p.adjust
HALLMARK_TNFA_SIGNALING_VIA_NFKB	119	0.667931	2.904656	5E-15
HALLMARK_E2F_TARGETS	136	-0.54067	-2.48075	1.03E-10
HALLMARK_P53_PATHWAY	115	0.577276	2.510132	4.66E-10
HALLMARK_MYC_TARGETS_V1	120	-0.49632	-2.21851	3.6E-07
HALLMARK_APOPTOSIS	95	0.533955	2.212198	9.73E-07
HALLMARK_TGF_BETA_SIGNALING	35	0.607185	2.068581	0.000279
HALLMARK_ANGIOGENESIS	20	0.694228	2.041837	0.000432
HALLMARK_OXIDATIVE_PHOSPHORYLATION	113	-0.38531	-1.70004	0.002105
HALLMARK_FATTY_ACID_METABOLISM	95	-0.39027	-1.66791	0.003631
HALLMARK_DNA_REPAIR	98	-0.35092	-1.51105	0.018524

TABLE 10: List of top 10 Hallmark Gene Sets Associated with Cancer

ID	setSize	enrichmentScore	NES	p.adjust
KEGG_LYSOSOME	78	0.586308	2.38161	1.95E-08
KEGG_TYROSINE_METABOLISM	19	-0.75803	-2.26587	6.24E-06
KEGG_FATTY_ACID_METABOLISM	28	-0.6442	-2.16986	3.38E-05
KEGG_DNA_REPLICATION	30	-0.63156	-2.15407	3.92E-05
KEGG_PPAR_SIGNALING_PATHWAY	34	-0.60339	-2.11504	7.81E-05
KEGG_GLYCOLYSIS_GLUCONEOGENESIS	34	-0.56538	-1.98181	0.000438
KEGG_REGULATION_OF_ACTIN_CYTOSKELETON	96	0.383716	1.61201	0.005178
KEGG_TGF_BETA_SIGNALING_PATHWAY	36	0.492041	1.676237	0.009378
KEGG_REGULATION_OF_AUTOPHAGY	16	0.615347	1.74437	0.015771
KEGG_ABC_TRANSPORTERS	18	-0.47312	-1.39309	0.103659

TABLE 11: List of top 10 KEGG gene sets Associated with Cancer

ID	setSize	enrichmentScore	NES	p.adjust
WP_TGFBETA_SIGNALING_PATHWAY	83	0.531992	2.157758	0.000254
WP_EGFEGFR_SIGNALING_PATHWAY	94	0.431547	1.786686	0.011468
WP_TH17_CELL_DIFFERENTIATION_PATHWAY	22	0.585232	1.784899	0.047179
WP_HEPATOCYTE_GROWTH_FACTOR_RECEPTOR_SIGNALING	19	0.603997	1.765068	0.047179
WP_VEGFAVEGFR2_SIGNALING	245	0.344664	1.648902	0.005612
WP_FOXA2_PATHWAY	15	-0.74324	-2.06278	0.005612
WP_DNA_REPLICATION	27	-0.62609	-2.07975	0.005612
WP_PPAR_SIGNALING_PATHWAY	33	-0.61093	-2.13745	0.002868
WP_DNA_REPAIR_PATHWAYS_FULL_NETWORK	75	-0.51847	-2.14778	0.000254

WP_AMINO_ACID_METABOLISM	57	-0.62581	-2.46147	4.54E-06

TABLE 12: List of top 10 Wiki Pathways gene sets Associated with Cancer

ID	setSize	enrichmentScore	NES	pvalue	p.adjust
STK33_UP	150	0.603129	2.711349	3.16E-16	5.82E-14
STK33_NOMO_UP	147	0.580118	2.600415	2.46E-14	2.26E-12
PDGF_ERK_DN.V1_DN	81	0.545347	2.214733	6.34E-07	2.91E-05
TGFB_UP.V1_UP	93	0.505988	2.09656	1.72E-06	4.82E-05
P53_DN.V1_UP	97	0.465446	1.944335	2.7E-05	0.000383
PKCA_DN.V1_DN	66	-0.42213	-1.68202	0.003772	0.016467
MYC_UP.V1_UP	80	-0.45056	-1.84088	9.89E-05	0.000867
RB_DN.V1_UP	71	-0.46176	-1.85516	0.000338	0.002302
PKCA_DN.V1_UP	63	-0.50044	-1.98097	8.2E-05	0.000838
PRC1_BMI_UP.V1_DN	58	-0.52053	-2.01467	2.66E-05	0.000383

TABLE 13: List of top 10 Oncogenic gene sets Associated with Cancer

6. Quantitative Real-Time PCR Validating of RNA Sequencing Data

To the validate RNA sequencing results and further investigate the expression patterns of genes associated with cancer, we selected 11 representative genes from the KEGG data for quantitative real-time PCR. The selected genes included mTOR signaling pathway [Frizzled class receptor 4(FZD4)], Galactose metabolism (AKR1B1), AMPK signaling pathway (PFKFB4), DNA replication pathway (MCM6, Glycine, serine and threonine metabolism(ADH4) [Alcohol dehydrogenase 4 (class II)], Complement and coagulation cascades[Serpin family E member 2(SERPINE2)], Ferroptosis [Acyl-CoA synthetase long-chain family member 4 (ACSL4)], Carbon metabolism[Isocitrate dehydrogenase 1 (NADP+) (IDH1)], Glycolysis / Gluconeogenesis [Hexokinase 2 (HK2)], PPAR signaling pathway [Acyl-CoA oxidase 2 (ACOX2)], and Fatty acid metabolism [Carnitine palmitoyltransferase 2 (CPT2)]. The qRT-PCR results showed that bufalin treatment significantly upregulated SERPINE2 and AKR1B1 expression ($p < 0.05$) and significantly downregulated ACOX2, ACSL4, FZD4, IDH1, PFKFB4, MCM6, ADH4, CPT2, and HK2 expression ($p < 0.05$) in HepG2 cells (Figure 6). These findings were consistent with the RNA sequencing results, indicating that bufalin modulates the expression of genes involved in various cellular processes that are implicated in hepatocellular carcinoma development and progression.

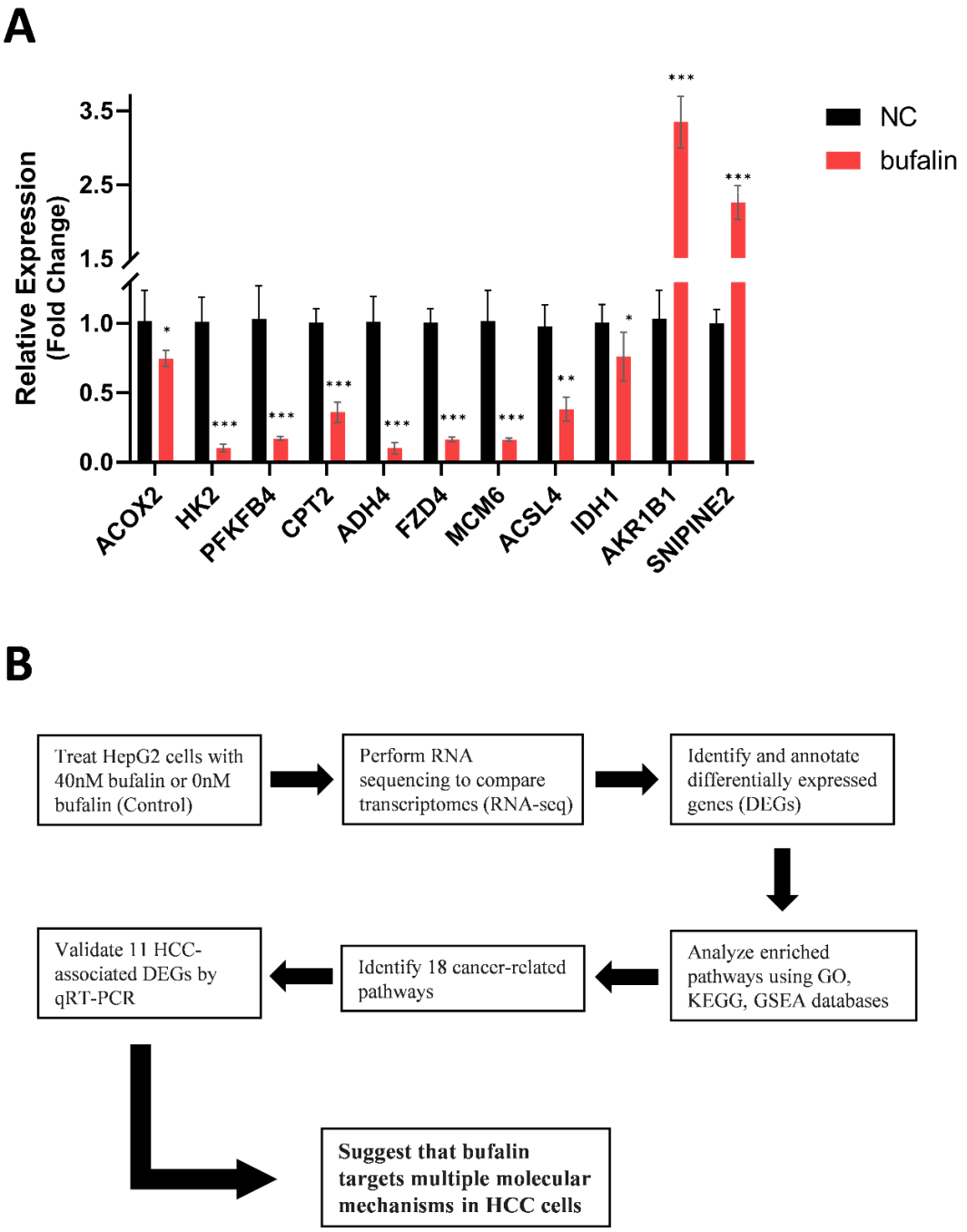

Figure 6: (A) qRT-PCR was performed in triplicate to validate the RNA sequencing results for 11 DEGs in HepG2 cells treated with 40 nM bufalin. GAPDH was used as a reference gene. The comparative threshold cycle (Ct) method was used to analyze the data. ***$p < 0.001$, **$p < 0.01$, *$p < 0.05$ versus control (NC) without bufalin. (B) Flowchart for elucidating the molecular mechanisms of bufalin's antitumor effect on HCC cells.

7. Discussion

Liver Hepatocellular Carcinoma cell lines are widely used in anticancer drug screening and liver cell physiology research. Derived from the tissues of HCC patients, these cells have a complete set of genes and can be passaged relatively stably. The most widely used liver cell lines include Bel-7402, SMMC-7721, Huh-7 and HepG2. HepG2 is a well-differentiated human liver cancer cell line that can retain some liver-specific functions, such as plasma protein synthesis and secretion. HepG2 cells are also suitable for 3D cell culture models that can mimic the tumor architecture and microenvironment more efficiently than 2D monolayer systems. Moreover, HepG2 cells are not infected by hepatitis viruses, which can be confounding factors for liver cancer research. Therefore, HepG2 cells are a useful in vitro model system for the study of liver cancer biology and drug response, compared with other liver cancer lines.

Transcriptomics has been used to identify the molecular

underpinnings of drug action in cancer by investigating differentially expressed genes and their associated pathway networks. Herein, we performed transcriptome sequencing of HepG2 cells exposed to bufalin to elucidate its antitumor mechanism of action. We identified potential gene targets of bufalin and elucidated the underlying signaling pathways induced by bufalin. While further research is warranted to validate these findings, this study provides a novel perspective for functional validation in future clinical trials. Cancer is a complex process characterized by a myriad of genetic alterations. Analyzing the involvement of various signaling molecules in biological processes can help elucidate bufalin's antitumor mechanism. Transcriptomics revealed that bufalin significantly modulated the expression of numerous genes in HepG2 cells, suggesting their potential involvement in bufalin's antitumor effects. These genes included 2 upregulated and 9 downregulated genes in bufalin-treated HepG2 cells.

Transcriptomic data analysis revealed that bufalin modulated glycolipid metabolism, ferroptosis, and the proliferation and migration of HCC cells. Among the 11 characterised genes, nine were downregulated by bufalin, namely ACOX2, ACSL4, FZD4, IDH1, PFKFB4, MCM6, ADH4, CPT2 and HK2. Only two genes, AKR1B1 and SERPINE2, were upregulated by bufalin. ACOX2, CPT2, ADH4 and ACSL4 are key enzymes in lipid metabolism, and ACSL4 is also involved in ferroptosis30. ACOX2 is an important rate-limiting enzyme in the cellular peroxisome responsible for catalysing both branched-chain fatty acid oxidation and bile acid synthesis31. ACOX2 is associated with colorectal cancer and primary cardiac malignancies in humans32, 33. Moreover, ACOX2 promotes the proliferation of estrogen receptor-positive (ER+) breast cancer34. The CPT2 gene encodes carnitine palmitoyltransferase II, an enzyme involved in fatty acid oxidation35. CPT2 expression is elevated in patients with recurrent breast cancer, and its high expression is associated with a poorer prognosis in breast cancer patients36. ADH4 is an important member of the ADH family that metabolises a variety of substrates, including ethanol and retinol. It was found that the overall survival rate of HCC patients with low expression of ADH4 was significantly lower than that of HCC patients with high expression37. ACSL4 is highly expressed in smooth muscle sarcoma, fibrosarcoma and rhabdomyosarcoma38. This evidence suggests that bufalin can modulate lipid metabolism and further inhibit the development and progression of HCC.

Bufalin also affected glucose metabolism and the proliferation and migration of HCC cells. HK2 belongs to the hexokinase family and is the first rate-limiting enzyme in glycolysis, catalysing the conversion of glucose to glucose-6-phosphate. The up-regulation of HK2 in HCC tissues correlates with a poor prognosis in HCC patients, and HK2 exerts a radioresistance effect by attenuating apoptosis and promoting proliferation in HCC cell lines39. IDH1 is an enzyme involved in the reactions of the tricarboxylic acid cycle and is widely found in various tissues and cells of the human body. In glioma, IDH1 gene mutation is closely related to the prognosis of the tumor. Through a large number of clinical case studies, it can be found that IDH1 mutations present a more obvious survival advantage, with patients surviving significantly longer than mutation-negative patients40. The main function of PFKFB4 is to synthesise F-2, 6-BP, the most potent metabolic activator of PFK-1, to control glycolytic fluxes and to promote ATP production, thereby affecting tumor growth41. MCM6 is responsible for encoding lactase, and MCM6 is upregulated in a variety of malignancies and is considered a new diagnostic biomarker. MCM6 promotes intrahepatic cholangiocarcinoma progression through activation of E2F1-mediated EMT42. AKR1B1 is able to catalyse NADPH-dependent reduction reactions of various carbonyl-containing compounds. In breast cancer, AKR1B1 expression is induced by the cellular transcription factor Twist2. Twist2 is known to play a critical role in EMT, and AKR1B1 then increases Twist2 levels by producing prostaglandin F2, which activates the NF-B signalling pathway43. bufalin further regulates the reaction process of glucose metabolism through key enzymes of glucose metabolism and inhibits the development of HCC.

In addition, bufalin further inhibited the proliferation and migration of HCC by affecting proliferation and migration-related proteins. FZD4 belongs to the Frizzled gene family, which family encodes for seven transmembrane regions of coiled-coil transmembrane receptor proteins, receptors for Wnt pathway signalling proteins that regulate cancer proliferation. The expression of FZD4 was significantly up-regulated in bladder cancer tissues and cell lines44. Overexpression of FZD4 promotes the ability of bladder cancer cells to migrate and invade44. SERPINE2 is inextricably linked to energy metabolism in the onset, progression and metastasis of cancer. SERPINE2 is an inhibitor of fibrinogen, urokinase and thrombin, which has been shown to correlate with tumourigenesis and tumour cell invasion and is also commonly up-regulated in lung, colon and pancreatic cancers45. SERPINE2 is an inhibitor of fibrinogen, urokinase, and thrombin, which has been shown to correlate with tumourigenesis and tumour cell invasion45, 46.

In conclusion, our study demonstrated that bufalin has potent anti-tumor effects on HCC cells by modulating multiple pathways and processes related to glycolipid metabolism, ferroptosis, proliferation, migration, and EMT. Given the promising results of this study, bufalin emerges as a potential therapeutic candidate for HCC, particularly for patients with drug resistance or poor prognosis. However, further investigation is warranted to elucidate the molecular underpinnings of bufalin's antitumor activity, evaluate its safety and efficacy in preclinical and clinical settings, and explore its potential synergistic effects with other anticancer agents [29-46].

8. Conclusion

Bufalin demonstrated potent antitumor activity against HepG2 HCC cells in vitro, inhibiting proliferation, migration, and invasion. This effect was mediated by a variety of pathways, including DNA replication, cell cycle, ferroptosis, glycolysis/gluconeogenesis, AMPK signaling, galactose metabolism, TNF signaling, carbon metabolism, TGF-β signaling, glycine, fatty acid metabolism, threonine metabolism and serine. Multiple genes related to cell cycle, cell adhesion, cell proliferation, substance metabolism and microRNAs in cancer were also

involved, such as HK2 , SERPINE2, ACOX2, ACSL4, FZD4, IDH1, PFKFB4, AKR1B1, ADH4, CPT2, and MCM family members.

In conclusion, this work suggests that bufalin may have therapeutic potential for liver cancer. However, further investigation is needed tovalidate these findings in other HCC cell lines and in vivo animal models. This work could pave the way for new and more effective liver cancer treatment strategies.

References

1. Llovet, J. M., Zucman-Rossi, J., Pikarsky, E., Sangro, B., Schwartz, M., Sherman, M., & Gores, G. (2016). Hepatocellular carcinoma. *Nature reviews. Disease primers 2*, 16018.
2. Bray, F., Ferlay, J., Soerjomataram, I., Siegel, R. L., Torre, L. A., & Jemal, A. (2018). Global cancer statistics 2018: GLOBOCAN estimates of incidence and mortality worldwide for 36 cancers in 185 countries. CA: *a cancer journal for clinicians, 68*(6), 394-424.
3. Farazi, P. A., & DePinho, R. A. (2006). Hepatocellular carcinoma pathogenesis: from genes to environment. *Nature Reviews Cancer, 6*(9), 674-687.
4. El–Serag, H. B., & Rudolph, K. L. (2007). Hepatocellular carcinoma: epidemiology and molecular carcinogenesis. *Gastroenterology, 132*(7), 2557-2576.
5. Yi, S. W., Choi, J. S., Yi, J. J., Lee, Y. H., & Han, K. J. (2018). Risk factors for hepatocellular carcinoma by age, sex, and liver disorder status: a prospective cohort study in Korea. *Cancer, 124*(13), 2748-2757.
6. Llovet, J. M., Ricci, S., Mazzaferro, V., Hilgard, P., Gane, E., Blanc, J. F., ... & Bruix, J. (2008). Sorafenib in advanced hepatocellular carcinoma. *New England journal of medicine, 359*(4), 378-390.
7. Abou-Alfa, G. K., Meyer, T., Cheng, A. L., El-Khoueiry, A. B., Rimassa, L., Ryoo, B. Y., ... & Kelley, R. K. (2018). Cabozantinib in patients with advanced and progressing hepatocellular carcinoma. *New England Journal of Medicine, 379*(1), 54-63.
8. Bruix, J., Qin, S., Merle, P., Granito, A., Huang, Y. H., Bodoky, G., ... & Han, G. (2017). Regorafenib for patients with hepatocellular carcinoma who progressed on sorafenib treatment (RESORCE): a randomised, double-blind, placebo-controlled, phase 3 trial. *The Lancet, 389*(10064), 56-66.
9. Kudo, M., Finn, R. S., Qin, S., Han, K. H., Ikeda, K., Piscaglia, F., ... & Cheng, A. L. (2018). Lenvatinib versus sorafenib in first-line treatment of patients with unresectable hepatocellular carcinoma: a randomised phase 3 non-inferiority trial. *The Lancet, 391*(10126), 1163-1173.
10. Farooqi, A. A., Rakhmetova, V. S., Kapanova, G., Tashenova, G., Tulebayeva, A., Akhenbekova, A., ... & Xu, B. (2023). Bufalin-Mediated Regulation of Cell Signaling Pathways in Different Cancers: Spotlight on JAK/STAT, Wnt/β-Catenin, mTOR, TRAIL/TRAIL-R, and Non-Coding RNAs. *Molecules, 28*(5), 2231.
11. Lan, Y. L., Lou, J. C., Jiang, X. W., Wang, X., Xing, J. S., Li, S., & Zhang, B. (2019). A research update on the anticancer effects of bufalin and its derivatives. Oncology letters, 17(4), 3635-3640.
12. Soumoy, L., Ghanem, G. E., Saussez, S., & Journe, F. (2022). Bufalin for an innovative therapeutic approach against cancer. *Pharmacological Research,* 106442.
13. Chen, G., Zhang, H., Sun, H., Ding, X., Liu, G., Yang, F., ... & Yang, L. (2023). Bufalin targeting BFAR inhibits the occurrence and metastasis of gastric cancer through PI3K/AKT/mTOR signal pathway. *Apoptosis*, 1-16.
14. Miao, Q., Bi, L. L., Li, X., Miao, S., Zhang, J., Zhang, S., ... & Wang, S. W. (2013). Anticancer effects of bufalin on human hepatocellular carcinoma HepG2 cells: roles of apoptosis and autophagy. *International journal of molecular sciences, 14*(1), 1370-1382.
15. Chen, F., Zhu, L., Hu, J., Jiang, S., Liu, H., Zheng, J., ... & Li, Z. (2020). Bufalin attenuates triple negative breast cancer cell stemness by inhibiting the expression of SOX2/OCT4. *Oncology Letters, 20*(5), 1-1.
16. Yu, Z., Li, Y., Li, Y., Zhang, J., Li, M., Ji, L., ... & Feng, H. (2022). Bufalin stimulates antitumor immune response by driving tumor-infiltrating macrophage toward M1 phenotype in hepatocellular carcinoma. *Journal for Immunotherapy of Cancer, 10*(5).
17. Xie, C. M., Chan, W. Y., Yu, S., Zhao, J., & Cheng, C. H. (2011). Bufalin induces autophagy-mediated cell death in human colon cancer cells through reactive oxygen species generation and JNK activation. *Free Radical Biology and Medicine, 51*(7), 1365-1375.
18. Gopal, R., Selvarasu, K., Pandian, P. P., & Ganesan, K. (2017). Integrative transcriptome analysis of liver cancer profiles identifies upstream regulators and clinical significance of ACSM3 gene expression. *Cellular oncology, 40*, 219-233.
19. Huang, C. J., Zhang, C. Y., Zhao, Y. K., Wang, D., Zhuang, L., Qian, L., ... & Meng, Z. Q. (2023). Bufalin Inhibits Tumorigenesis and SREBP-1-Mediated Lipogenesis in Hepatocellular Carcinoma via Modulating the ATP1A1/CA2 Axis. *The American Journal of Chinese Medicine, 51*(02), 461-485.
20. Jiang, Y., Zhang, Y., Luan, J., Duan, H., Zhang, F., Yagasaki, K., & Zhang, G. (2010). Effects of bufalin on the proliferation of human lung cancer cells and its molecular mechanisms of action. *Cytotechnology, 62*, 573-583.
21. Ding, D. W., Zhang, Y. H., Huang, X. E., An, Q., & Zhang, X. (2015). Bufalin induces mitochondrial pathway-mediated apoptosis in lung adenocarcinoma cells. *Asian Pacific Journal of Cancer Prevention, 15*(23), 10495-10500.
22. Tian, X., Dai, S., Sun, J., Jiang, S., Sui, C., Meng, F., ... & Jiang, Y. (2015). Bufalin induces mitochondria-dependent apoptosis in pancreatic and oral cancer cells by downregulating hTERT expression via activation of the JNK/p38 pathway. *Evidence-Based Complementary and Alternative Medicine,* 2015.
23. Li, Y., Tian, X., Liu, X., & Gong, P. (2018). Bufalin inhibits human breast cancer tumorigenesis by inducing cell death through the ROS-mediated RIP1/RIP3/PARP-1 pathways. *Carcinogenesis, 39*(5), 700-707.
24. Dou, L., Zou, D., Song, F., Jin, Y., Li, Y., & Zhang, Y.

(2022). Bufalin suppresses ovarian cancer cell proliferation via EGFR pathway. *Chinese Medical Journal, 135*(04), 456-461.
25. Zhang, J. J., Zhou, X. H., Zhou, Y., Wang, Y. G., Qian, B. Z., He, A. N., ... & Yao, Y. (2019). Bufalin suppresses the migration and invasion of prostate cancer cells through HOTAIR, the sponge of miR-520b. *Acta Pharmacologica Sinica, 40*(9), 1228-1236.
26. Zhu, Z., Li, E., Liu, Y., Gao, Y., Sun, H., Wang, Y., ... & Liu, Y. (2012). Bufalin induces the apoptosis of acute promyelocytic leukemia cells via the downregulation of survivin expression. *Acta Haematologica, 128*(3), 144-150.
27. Wu, T., Hu, E., Xu, S., Chen, M., Guo, P., Dai, Z., ... & Yu, G. (2021). clusterProfiler 4.0: A universal enrichment tool for interpreting omics data. *The innovation, 2*(3).
28. Jiang, H. Y., Zheng, H. M., Xia, C., Li, X., Wang, G., Zhao, T., ... & Liu, Y. (2022). The Research Progress of Bufalin in the Treatment of Hepatocellular Carcinoma. *OncoTargets and therapy*, 291-298.
29. Abaan, O. D., Polley, E. C., Davis, S. R., Zhu, Y. J., Bilke, S., Walker, R. L., ... & Meltzer, P. S. (2013). The exomes of the NCI-60 panel: a genomic resource for cancer biology and systems pharmacology. *Cancer research, 73*(14), 4372-4382.
30. Ding, K., Liu, C., Li, L., Yang, M., Jiang, N., Luo, S., & Sun, L. (2023). Acyl-CoA synthase ACSL4: an essential target in ferroptosis and fatty acid metabolism. *Chinese Medical Journal, 136*(21), 2521-2537.
31. Sui, J. S., Martin, P., Keogh, A., Murchan, P., Ryan, L., Nicholson, S., ... & Gray, S. G. (2022). Altered expression of ACOX2 in non-small cell lung cancer. *BMC Pulmonary Medicine, 22*(1), 1-21.
32. Yeh, C. S., Wang, J. Y., Cheng, T. L., Juan, C. H., Wu, C. H., & Lin, S. R. (2006). Fatty acid metabolism pathway play an important role in carcinogenesis of human colorectal cancers by Microarray-Bioinformatics analysis. *Cancer letters, 233*(2), 297-308.
33. Zhou, X., & Wang, H. (2017). ACOX2 deficiency in primary malignant cardiac tumors. *Proceedings of the National Academy of Sciences, 114*(18), E3590-E3591.
34. Bjørklund, S. S., Kristensen, V. N., Seiler, M., Kumar, S., Alnæs, G. I. G., Ming, Y., ... & Ganesan, S. (2015). Expression of an estrogen-regulated variant transcript of the peroxisomal branched chain fatty acid oxidase ACOX2 in breast carcinomas. *BMC cancer, 15*(1), 1-13.
35. Isackson, P. J., Sutton, K. A., Hostetler, K. Y., & Vladutiu, G. D. (2013). Novel mutations in the gene encoding very long-chain acyl-CoA dehydrogenase identified in patients with partial carnitine palmitoyltransferase ii deficiency. *Muscle & nerve, 47*(2), 224-229.
36. Han, S., Wei, R., Zhang, X., Jiang, N., Fan, M., Huang, J. H., ... & Li, J. J. (2019). CPT1A/2-mediated FAO enhancement—a metabolic target in radioresistant breast cancer. *Frontiers in Oncology, 9,* 1201.
37. Wei, R. R., Zhang, M. Y., Rao, H. L., Pu, H. Y., Zhang, H. Z., & Wang, H. Y. (2012). Identification of ADH4 as a novel and potential prognostic marker in hepatocellular carcinoma. *Medical Oncology, 29*, 2737-2743.
38. Yang, Y., Zhu, T., Wang, X., Xiong, F., Hu, Z., Qiao, X., ... & Wang, D. (2022). ACSL3 and ACSL4, distinct roles in ferroptosis and cancers. *Cancers, 14*(23), 5896.
39. Zheng, Y., Zhan, Y., Zhang, Y., Zhang, Y., Liu, Y., Xie, Y., ... & Fang, Y. (2023). Hexokinase 2 confers radio-resistance in hepatocellular carcinoma by promoting autophagy-dependent degradation of AIMP2. *Cell Death & Disease, 14*(8), 488.
40. Platten, M., Bunse, L., Wick, A., Bunse, T., Le Cornet, L., Harting, I., ... & Wick, W. (2021). A vaccine targeting mutant IDH1 in newly diagnosed glioma. *Nature, 592*(7854), 463-468.
41. Gao, R., Li, D., Xun, J., Zhou, W., Li, J., Wang, J., ... & Luo, N. (2018). CD44ICD promotes breast cancer stemness via PFKFB4-mediated glucose metabolism. *Theranostics, 8*(22), 6248.
42. Gao, C., Li, J., Zeng, F., Wang, L., Chen, K., Chen, D., ... & Qu, C. (2023). MCM6 promotes intrahepatic cholangiocarcinoma progression by upregulating E2F1 and enhancing epithelial–mesenchymal transition. *Carcinogenesis, 44*(4), 279-290.
43. Wu, X., Li, X., Fu, Q., Cao, Q., Chen, X., Wang, M., ... & Dong, C. (2017). AKR1B1 promotes basal-like breast cancer progression by a positive feedback loop that activates the EMT program. *Journal of Experimental Medicine, 214*(4), 1065-1079.
44. Chen, L., Long, Y., Han, Z., Yuan, Z., Liu, W., Yang, F., ... & Zhong, Y. (2019). MicroRNA 101 inhibits cell migration and invasion in bladder cancer via targeting FZD4. *Experimental and Therapeutic Medicine, 17*(2), 1476-1485.
45. Zhang, J., Wu, Q., Zhu, L., Xie, S., Tu, L., Yang, Y., ... & Zhang, S. (2022). SERPINE2/PN-1 regulates the DNA damage response and radioresistance by activating ATM in lung cancer. *Cancer Letters, 524,* 268-283.
46. Wang, K., Wang, B., Xing, A. Y., Xu, K. S., Li, G. X., & Yu, Z. H. (2015). Prognostic significance of SERPINE2 in gastric cancer and its biological function in SGC7901 cells. *Journal of cancer research and clinical oncology, 141,* 805-812.